
**Liquid Crystals**
Publication details, including instructions for authors and subscription information:
http://www.informaworld.com/smpp/title~content=t713926090

# Frequency response due to the orientational motion of the director around the smectic cone in a surface stabilized ferroelectric liquid crystal

Muklesur Rahman[a]; S. S. Bhattacharyya[a]; B. K. Chaudhuri[a]
[a] Department of Solid State Physics, Indian Association for the Cultivation of Science, Kolkata-700032, India

**To cite this Article** Rahman, Muklesur , Bhattacharyya, S. S. and Chaudhuri, B. K.(2006) 'Frequency response due to the orientational motion of the director around the smectic cone in a surface stabilized ferroelectric liquid crystal', Liquid Crystals, 33: 10, 1207 — 1214
**To link to this Article: DOI:** 10.1080/02678290601020021
**URL:** http://dx.doi.org/10.1080/02678290601020021

*Liquid Crystals*, Vol. 33, No. 10, October 2006, 1207–1214

Taylor & Francis
Taylor & Francis Group

# Frequency response due to the orientational motion of the director around the smectic cone in a surface stabilized ferroelectric liquid crystal

MUKLESUR RAHMAN, S.S. BHATTACHARYYA and B.K. CHAUDHURI*
Department of Solid State Physics, Indian Association for the Cultivation of Science, Kolkata-700032, India

(*Received 13 February 2006; in final form 3 August 2006; accepted 12 August 2006*)

We report the effects of the rotational motion of the director around the chiral smectic cone on the dielectric relaxation and polarization reversal process in a surface stabilized ferroelectric liquid crystal cell. Measurement was made at a fixed temperature (40°C), far below the SmA–SmC* transition temperature (62°C) of the ferroelectric liquid crystal material (CS-1027). The amount of switchable polarization (ASP), during the polarization reversal, is found to decrease with increasing frequency of the applied signal until a typical value of frequency ($f_i$) is reached. This behaviour is considered to be due to the time-dependent rotational motion of the director. The ASP value was calculated by measuring polarization–voltage (P–V) and capacitance–voltage (C–V) hysteresis loops as a function of the applied signal frequency and then following the Preisach model for the ferroelectric capacitor. The peaks of the C–V hysteresis loop, which correspond to the reversal of polarization, are gradually converted into wells for frequencies greater than a critical value ($f_i$). The hysteresis loops shows 'frustrated' behaviour for frequencies between $f_i$ and $f_i$. The inversion of the C–V hysteresis loop at higher frequencies ($>f_i$) is attributed to the inversion of the dielectric biaxiality and the corresponding 'frustrated' behaviour arising due to competition between the dielectric and ferroelectric torques. A suitable equivalent circuit can be designed to represent the frequency-dependent C–V and magnitude of admittance (conductance) –voltage (G–V) hysteresis behavior.



## 1. Introduction

Following the discovery of ferroelectricity in tilted chiral smectic phases by Meyer *et al.* [1], research has focussed particularly on the chiral smectic C (SmC*) phase because of its applications in electro-optical devices. Tilted smectic phases, having biaxial symmetry, exhibit dielectric biaxiality $\partial\varepsilon=\varepsilon_2-\varepsilon_1$, where $\varepsilon_2$ is the component of the dielectric permittivity ($\varepsilon$) normal to the director and to the tilted plane, and $\varepsilon_1$ is the component normal to the director and $\varepsilon_2$ [2, 3]. Frequency- and temperature-dependent behaviour of $\partial\varepsilon$ has been well studied [3–5]. In the tilted phases, chiral molecules exhibit spontaneous polarization ($\mathbf{P}_S$) in the direction of $\varepsilon_2$ due to a time-dependent coupling between the lateral components of the dipoles of the individual molecules and the chiral environment. But due to the helicoidal structure of the layers, with the helical axis coinciding with the layer normal, $\mathbf{P}_S$ also precesses from layer to layer and forms a helix so that there is no macroscopic polarization. The helix formation can be prevented by introducing parallel boundary surfaces, normal to the layer. This is the basis of the surface stabilized ferroelectric liquid crystal (SSFLC) [6].

SSFLC cells generally exhibit chevron layer structure [7]. In a ferroelectric liquid crystal, the dielectric relaxation phenomenon reflects the delay (time dependence) in the frequency response of a group of dipoles subjected to an external electric field, because the polarization vector (or director) cannot always follow the variation of the alternating field. Due to the fluctuation in the azimuthal orientation of the director, the Goldstone (G) mode appears in the SmC* phase relaxation spectra [8]. The G-mode contribution can also be destroyed by applying an external bias field [9–11]. If there is relaxation of the molecules, the polarization reversal method may be affected by the signal frequency. Considering uniform director rotation around the smectic cone, Reynaerts and DeVos [12] demonstrated the frequency dependence of the polarization voltage (**P**–*V*) hysteresis loop. The orientation of the chiral molecules around the smectic cone of the SSFLC is governed by both the dielectric torque ($\sim\mathbf{E}^2$)

*Corresponding author. Email: sspbkc@iacs.res.in

*Liquid Crystals*
ISSN 0267-8292 print/ISSN 1366-5855 online © 2006 Taylor & Francis
http://www.tandf.co.uk/journals
DOI: 10.1080/02678290601020021

and the ferroelectric torque ($\sim$**E**), for the applied field **E** along the polarization axis [13]. The molecules can be made to align parallel or anti-parallel to the positive field direction. Transition from the anti-parallel state to the parallel state is followed by a change in the direction of polarization. Thus the capacitance changes with bias as the dielectric constant changes with the d.c. bias ($\varepsilon \propto d\mathbf{P}(V)/dV$), resulting in a $C$–$V$ hysteresis loop. As pointed out by Yang *et al.* [14] and Miller *et al.* [15], the peaks of the $C$–$V$ hysteresis of the ferroelectric capacitor correspond to the reversal of polarization, and the peak intensity corresponds to the amount of switchable polarization. The $C$–$V$ hysteresis loop measures the d.c. field dependence of the dielectric constant, which is a widespread method for examining the behaviour of ferroelectric materials [16]. Ferroelectric materials also exhibit hysteresis behaviour in $G$–$V$ characteristics. These characteristics of ferroelectric materials are generally measured by applying a small a.c. field across the sample while the d.c. field is swept in an itinerary of $-V_{max}$ to $+V_{max}$ and $+V_{max}$ to $-V_{max}$.

In this paper we have analysed the effects of the rotational motion of the director on the dielectric relaxation and polarization reversal phenomena. Considering the orientation of the FLC molecule around the smectic cone, and using the Preisach model [17, 18] for ferroelectric capacitor, we showed gradual decrease in the amount of switchable polarization (ASP) with increasing number of polarizing cycle, and inversion of the $C$–$V$ hysteresis loop at higher frequencies. The frequency dependences of the $G$–$V$ and $C$–$V$ hysteresis loops have been related by considering a suitable electrical equivalent for the FLC capacitor. The material selected for these studies is a ferroelectric liquid crystal mixture, CS-1027, obtained from the Chisso Corporation, Japan. This material possesses a spontaneous polarization (25.5 nC cm$^{-2}$ at 40.0°C) and the phase sequence Cr–13.0°C–SmC*–62.0°C–SmA–88.0°C– N*–96.0°C—I.

## 2. Experimental

A shielded parallel plate condenser of 3 μm thickness and 16 μm$^2$ active area was used for the present measurements. Indium tin oxide (ITO) coated transparent glass substrates were used as electrodes. Substrates were prepared by coating the glass plates with polyvinyl alcohol (PVA) and baking at 130.0°C for 2 h. Homogeneously aligned samples were obtained by rubbing the substrates in one direction. The temperature of the FLC cell was controlled using a Eurotherm controller with an accuracy of ±0.1°C. Measurements were performed at a fixed temperature of 40.0°C in the SmC* phase. Dielectric measurements were carried out by a computer-controlled HP 4192A impedance analyser having a bias voltage range ±35 V and frequency range 5 Hz–13 MHz. The $C$–$V$ and $G$–$V$ measurements were performed with bias voltage −5 V (minimum) to +5 V (maximum) with an 0.1 V step and then similarly reversed. The bias voltage was superimposed on a sinusoidal wave of amplitude 1.0 V. Figures 1 (*a*) and 1 (*b*) show the equivalent electrical circuits for the FLC. Dynamic hysteresis curves were obtained using the Sawyer–Tower (ST) method [19, 20]. The ST circuit shown in figure 1 (*c*) was constructed with a high precision signal generator (S) (FG200, Yokogawa), a high resolution storage oscilloscope (DL1720, 500 MHz, 1GS/s). A sinusoidal signal of amplitude 5 V was used to initiate the polarization reversal.

## 3. Results and discussion

### 3.1. *Dielectric relaxation*

Figure 2 (*a*) shows the frequency dependence of the real ($\varepsilon'$) and imaginary ($\varepsilon''$) parts of the dielectric permittivity measured at 40.0°C in the absence of bias. The solid

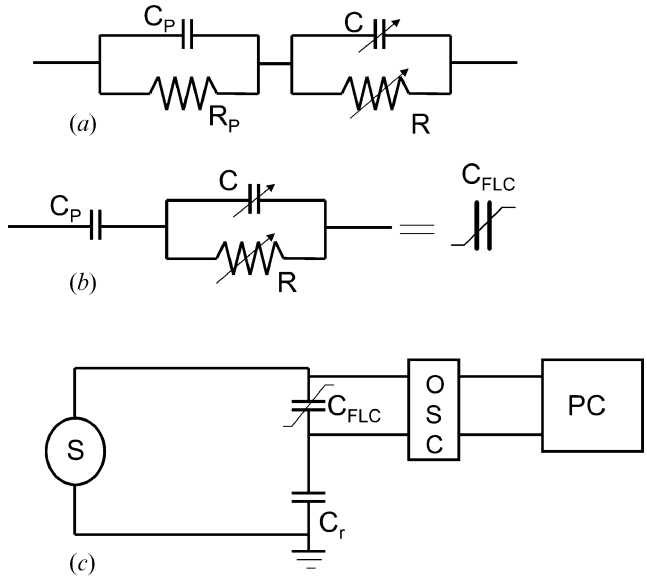


Figure 1. (*a*) Equivalent circuits for the SSFLC cell (capacitor) in which $C_P$ and $R_P$ are the permanent capacitance and resistance of the polymer layer, respectively; $R$ and $C$ correspond to the dynamic resistance and capacitance of the liquid crystal layer. (*b*) The same cell with resistance of polymer layer neglected. (*c*) Schematic diagram of ST circuit for **P**–$V$ hysteresis measurement. $S$ is the function generator, $C_r$ (=0.01 μF) is the reference capacitor. The oscilloscope was used in $XY$ mode.

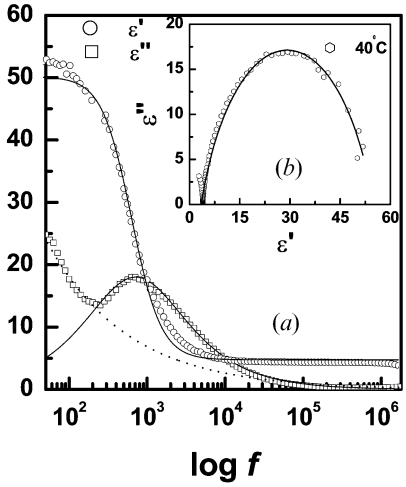


Figure 2. (*a*) Variation of the real ($\varepsilon'$) and imaginary ($\varepsilon''$) part of the dielectric constant of CS-1027 with frequency in the SmC* phase at a fixed temperature 40.0°C. The dotted line shows the conductivity contribution following equation (4) with the $\delta_0 = 1.129 \times 10^{-10}\,\text{ohm}^{-1}\,\text{cm}^{-1}$. (*b*) Corresponding Cole–Cole plot for the Goldstone mode in the SmC* phase under unbiased condition at 40.0°C.



lines indicate the fitted lines using the Debye formulae

$$\varepsilon'(\omega) = \varepsilon_\infty + (\varepsilon_S - \varepsilon_\infty)/(1+\omega^2\tau^2) \quad (1)$$

and

$$\varepsilon''(\omega) = (\varepsilon_S - \varepsilon_\infty)\omega\tau/(1+\omega^2\tau^2) \quad (2)$$

where $\varepsilon_S$ and $\varepsilon_\infty$ are the static and high frequency dielectric permittivity, respectively; $\omega$ is the angular frequency of the applied signal. The relaxation time $\tau$ is the inversion of relaxation $f_R$ and the relaxation peak frequency is given by $[1/2\pi f_R]$. If a dielectric exhibits a continuous distribution of relaxation time, it can be described by the Cole–Cole (C-C) distribution of relaxation time as [21]

$$\varepsilon^* = \varepsilon_\infty + \frac{\varepsilon_0 - \varepsilon_\infty}{\left[1-(i\omega\tau)^{1-\alpha}\right]} \quad (3)$$

where $\alpha$ is the relaxation parameter for a particular relaxation process. For a distribution of relaxation times, $\alpha$ varies from 0 to1.0. A corresponding C-C plot for the G-mode is shown in the figure 2 (*b*). At lower frequencies, there are contributions from the electrical conduction to the dielectric data. This contribution can be expressed by [22]

$$\varepsilon''(\omega) = \frac{\delta_0}{\varepsilon_0 \omega^{1-S}} \quad (4)$$

where $\varepsilon_0$ is the free space permittivity, $\delta_0$ and $S$ are the fitting parameters; the power law exponent ($S$) should be close to zero. In figure 2 (*a*), the dotted line represents the curve fitted with equation (4); the best fit parameters are $S=0.058$ and $\delta_0 = 1.129 \times 10^{-10}\,\text{ohm}^{-1}\,\text{cm}$. The effects of the external bias field on the dielectric spectra are shown in figures (3) and (4). It is visualized from these figures that the dielectric permittivity is maximum in the unbiased condition and decreases gradually with increasing bias field. In the absence of bias field, the large peak height in the ($\varepsilon''-f$) curve, figure 2 (*a*), arises due to the G-mode contribution. The said peak height decreases with increasing bias field. The relaxation frequency $f_R$ is almost constant at low bias voltage but starts to shift to the higher frequency side at a bias of ~3.4 V, figure 4 (*b*). It is also observed that by applying a bias>4.8 V, the relaxation could not be detected. The change of the relaxation parameter ($f_R$) with bias field is also attributed to the change in the helical structure of the SmC* phase [9–11].

### 3.2. *Polarization–voltage and capacitance–voltage hysteresis*

As mentioned above, in a SSFLC cell, the motion of the director moving on the smectic cone is subjected to ferroelectric and dielectric torques, so the dynamic

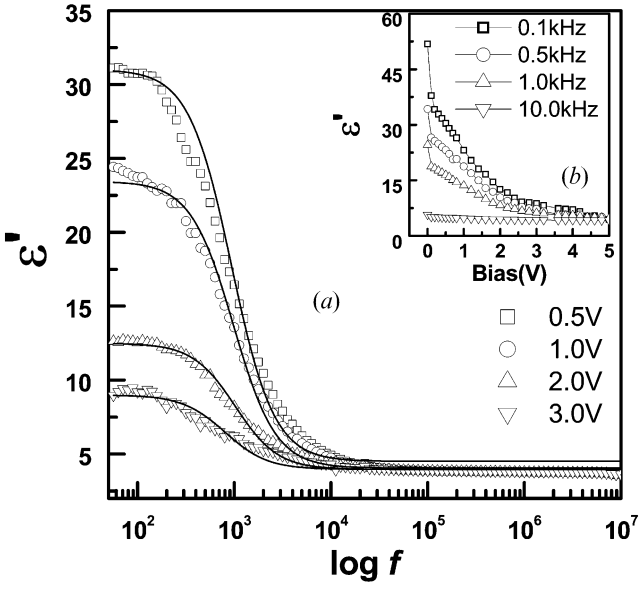


Figure 3. (*a*) Variation of the imaginary part of the dielectric constant ($\varepsilon'$) of CS-1027 with frequency at different bias voltages at a fixed temperature of 40.0°C. (*b*) Variation of $\varepsilon'$ with bias voltage for different frequencies.

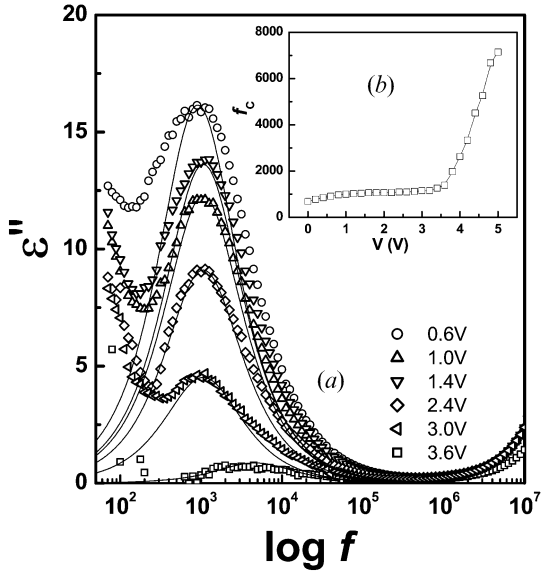


Figure 4. Variation of the imaginary part of the dielectric constant ($\varepsilon''$) in the SmC* phase of CS-1027 with frequency at different bias voltages at a fixed temperature 40.0°C. (*b*) Variation of the relaxation frequency of the SmC* phase with different bias voltages at 40.0°C.

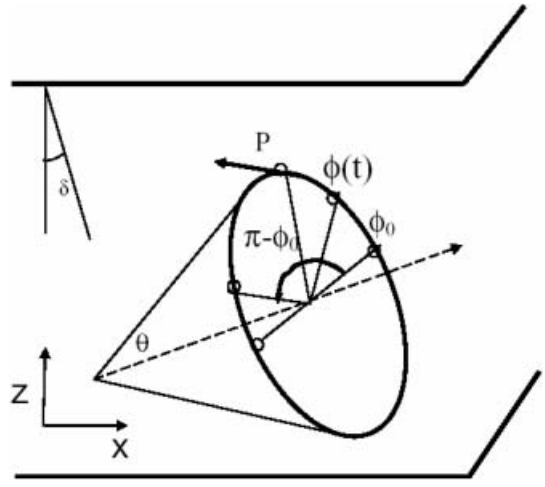


Figure 5. Orientation of the FLC molecule under external field; $\theta$, $\delta$ and $\phi_0$ are the tilt, layer tilt and pretilt angle respectively. The azimuthal angle $\phi$ switches between the states $\phi=\phi_0$ to fully switched state $\phi=\pi-\phi_0$. When the time period of the applied signal is high then the switching from these two states is completed and contributes fully to the polarization reversal. For signals with higher frequencies the switching does not reach completion and thus the amount of switchable polarization decreases.

director equation has the form

$$\eta\frac{\mathrm{d}\phi}{\mathrm{d}t}=\mathbf{P}_\mathrm{S}\,\mathbf{E}\cos\delta\sin\phi+\varepsilon_0\partial\varepsilon\,\mathbf{E}^2\cos^2\delta\sin\phi\cos\phi \quad (5)$$

where $\eta$ is the rotational viscosity so that $\eta\,\mathrm{d}\phi/\mathrm{d}t$ denotes the viscous torque, $d$ is the cell thickness and $\delta$ is the layer tilt angle [23]. However, under a sinusoidal electric voltage, $v(t)=V\sin\omega t$, it is reasonable to assume a uniform switching model so that the molecular reorientation process is described by a simple rotation around the SmC* cone (figure 5). Then the azimuthal angle $\phi$ satisfies the well known differential equation

$$\eta\frac{\mathrm{d}\phi}{\mathrm{d}t}=\mathbf{P}_\mathrm{S}\,\mathbf{E}\cos\delta\sin\phi. \quad (6)$$

The azimuthal angle $\phi$ switches between the states $\phi=\phi_0$ (pretilt, $0<\phi_0<\pi$) and fully switched state $\phi=\pi-\phi_0$. Figure 5 shows the orientation of the FLC molecule under an external signal around the smectic cone. From equation (6) one finds that for higher $\mathbf{P}_\mathrm{S}$ switching occurs more quickly. The solution of the differential equation (6) is

$$\phi(t)=2\tan^{-1}\left\{\tan\left(\frac{\phi_0}{2}\right)\exp\left[\frac{kV}{\omega}(1-\cos\omega t)\right]\right\} \quad (7)$$

where $k=\dfrac{\mathbf{P}_\mathrm{S}}{\eta d\cos\delta}$ and $\mathbf{E}=\dfrac{V}{d}$. The expression for polarization $\mathbf{P}(v)$ is given by [12]

$$\mathbf{P}(v)=\mathbf{P}_\mathrm{S}\frac{1-\tan^2\left(\frac{\phi_0}{2}\right)\exp\left\{\left(\frac{2k}{\omega}\right)\left[V\pm\left(V^2-v^2\right)^{\frac{1}{2}}\right]\right\}}{1+\tan^2\left(\frac{\phi_0}{2}\right)\exp\left\{\left(\frac{2k}{\omega}\right)\left[V\pm\left(V^2-v^2\right)^{\frac{1}{2}}\right]\right\}}$$

which shows a dependence of polarization on the time period of the applied signal.

In considering the effects of non-saturated loops, different authors assumed a tanh relationship between the polarization and the voltage [15, 24, 25], viz.

$$\mathbf{P}(V)=F\,\mathbf{P}_\mathrm{sat}\tanh\left[\beta\left(V\mp V_\mathrm{C}^{\pm}\right)\right] \quad (8)$$

where $V_\mathrm{C}{}^{\pm}$ is the macroscopic coercive voltage, i.e. the mean value of the individual coercive voltages of the molecules. The (+) and (−) signs are valid, respectively, for increasing and decreasing values of $V$. The behaviour of the non-saturated loops is taken into account by the factor $F$ so that ($F.\mathbf{P}_\mathrm{Sat}$) represents the ASP taking part in the polarization reversal process. If $\mathbf{P}_\mathrm{r}$ be the remnant polarization then the constant β is defined as

$$\beta=V_\mathrm{C}^{-1}\left[\log\left(\frac{1+x}{1-x}\right)\right] \quad (9)$$

where $x=\mathbf{P}_\mathrm{r}/\mathbf{P}_\mathrm{S}$ [15]. Figures 6 (*a–c*) show the $\mathbf{P}$–$V$ hysteresis loops generated by the ST circuit using a sine wave of 5 V amplitude for frequencies 1.0, 5.0 and

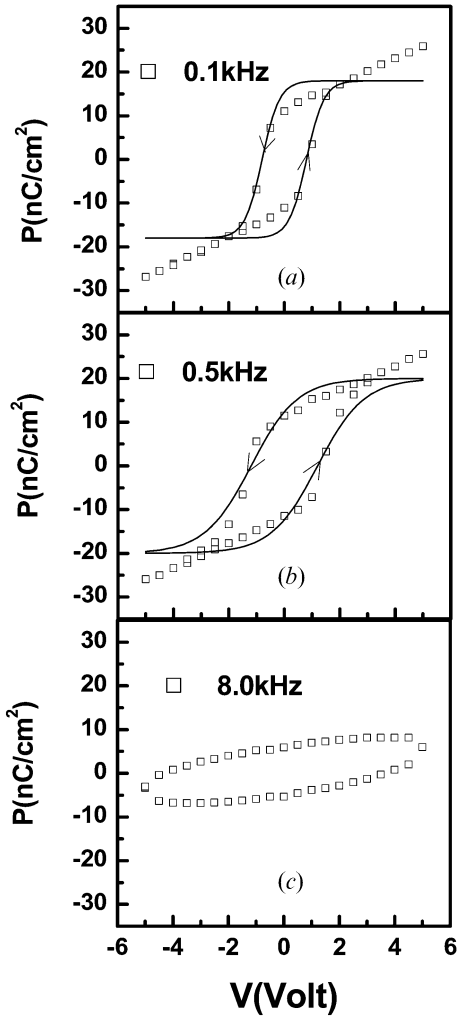


Figure 6. **P**–$V$ hysteresis loops for the frequency (*a*) 0.1 (*b*) 0.5 (*c*) 8.0 kHz, and in the SmC* phase at temperature 40.0°C generated by the ST circuit using a sine wave of 5 V amplitude. The solid lines represents the fitting curve with equation (8).

8.0 kHz, respectively, at temperature 40°C. The value of β, obtained from the fitting of the **P**–$V$ hysteresis with equation (8), is 0.931. At higher frequencies deformation in the shape of the **P**–$V$ hysteresis loops occur, as shown for a typical frequency 8.0 kHz in figure 6 (*c*). Such behaviour of the **P**–$V$ hysteresis loop has been explained by Reynarts and DeVos [12]; they could not calculate the ASP. Due to the variation of polarization with the applied field there is a non-linear contribution to the dielectric value of the ferroelectric material, so that the total value of the capacitance for a FLC capacitor becomes

$$C = C_{\mathrm{f}} + \left(\frac{\mathrm{d}\mathbf{P}}{\mathrm{d}V}\right)\frac{S}{L}$$

where $C_{\mathrm{f}}$ is the linear capacitance, $V$ is the applied voltage and $L$, $S$ are the thickness and area of the capacitor respectively [14]. The non-linear part of the capacitance (or dielectric constant) value is the contribution due to the polarization reversal under d.c. field. Differentiation of equation (8) with respect to $V$ gives

$$C = C_{\mathrm{f}} + \frac{F\,\mathbf{P}_{\mathrm{sat}}\,\beta}{\cosh^2\left[\beta\left(V \mp V_{\mathrm{C}}^{\pm}\right)\right]}\frac{S}{L}. \qquad (10)$$

Equation (9) for the $C$–$V$ hysteresis indicates two peaks corresponding to $V_{\mathrm{C}}{}^{\pm}$. The distance between the two peaks in the $C$–$V$ hysteresis loop is twice the coercive voltage. Figure 7 (*a*) shows the $C$–$V$ hysteresis loops for different frequencies (0.1, 0.5, 1.0 and 2.0 kHz). The continuous line in the plot of figure 7 (*b*), is obtained by fitting the experimental $C$–$V$ data with equation (10). The parameter β (=0.927) remains almost constant for all frequencies. Here it should be noted that there is some contribution to the capacitance value from the aligned layers, which we have not taken into consideration. Figure 7 (*a*) exhibits clearly a continuous decrease of peak intensity of the hysteresis loop with increasing frequency.

If there are relaxations of the molecules, a variation of the switchable part of the polarization with frequency is expected. This could be related to the director orientation of the FLC molecules under small signal. The process of director orientation under an applied a.c. field depends on the magnitude of the field as well as its frequency. As long as the period of the applied signal is high in comparison with the time required for the molecule to reach its final position $\phi(T)$ ($=\pi-\phi_0$, see figure 5), the effect of molecular motion is almost independent of the frequency of the a.c. field. At higher frequencies, the applied a.c. field changes direction before the molecule reaches the fully switched state for the said applied field magnitude. Hence the gradual increase in the switchable polarization ($F.\mathbf{P}_{\mathrm{sat}}$) with increase of time period is attributed to the motion of the director under the ferroelectric torque [12]. The variation of the amount of switchable polarization ($F.\mathbf{P}_{\mathrm{sat}}$) with frequency of the applied signal, obtained from fitting of the $C$–$V$ hysteresis data with equation (9), is shown in the figure 7 (*c*). The value of ($F.\mathbf{P}_{\mathrm{sat}}$) decreases with increasing signal frequency. From figure 4 it is seen that the contribution to the capacitance due to the G-mode at higher bias field and higher frequency is constant. Although it appears from figures 2 and 3 that the G-mode contribution to the dielectric constant is maximum at 0.0 V, in the $C$–$V$ hysteresis loop, peaks appear at the coercive voltages.

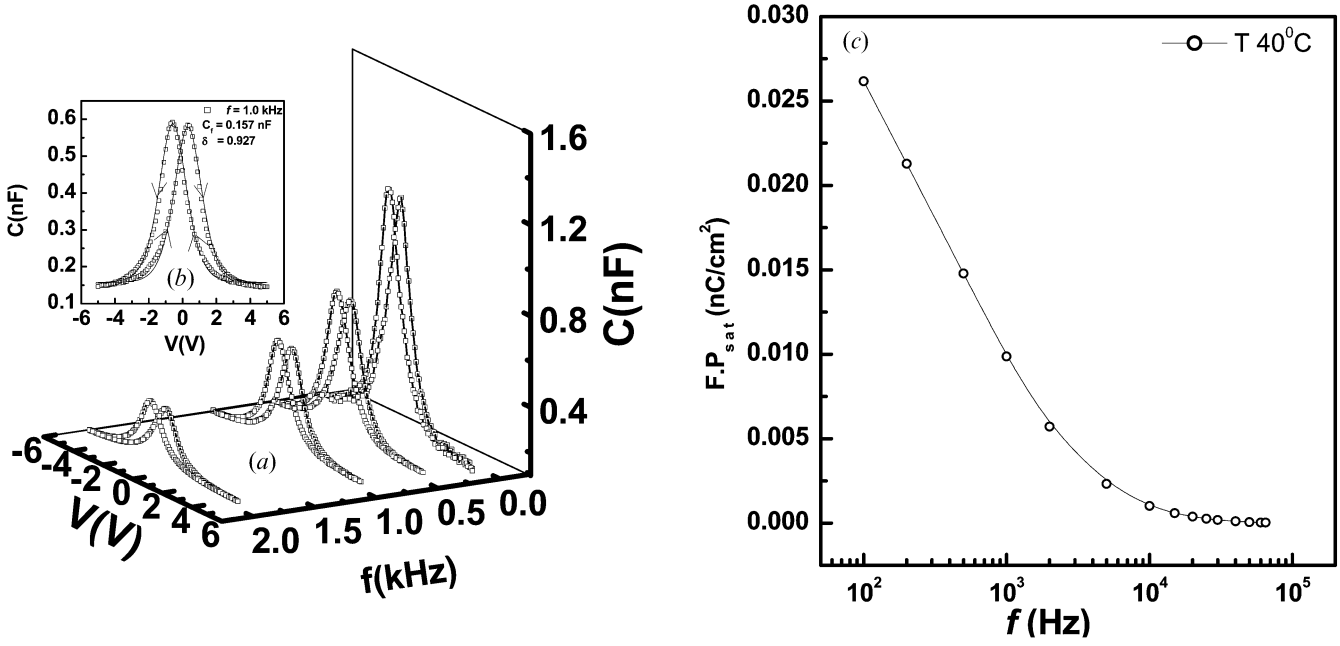


Figure 7. (*a*) *C–V* hysteresis curves for signal frequency (*f*) 0.1, 0.5, 1.0 and 2.0 kHz, showing the gradual decrease in peak intensity with increasing *f*. The d.c. bias swept from −5.0 Vto +5.0 V in steps of 0.1 V and then reversed. The decrease in peak height continues up to a frequency of 68.0 kHz. (*b*) *C–V* hysteresis loop at $f$=1.0 kHz which is symmetric corresponding to the point at zero bias. The solid line is the fitted line with equation (10) for β=0.927 (*c*) Decrease in the amount of switchable polarization ($F.\mathbf{P}_{sat}$) with increasing frequency (*f*), obtained from fitting the experimental *C–V* hysteresis loops with equation (9).



The FLC mixture CS-1027 of our present investigation exhibits a decrease of ($F.\mathbf{P}_{sat}$) with increasing frequency up to the signal frequency $f_l$=65.0 kHz. With

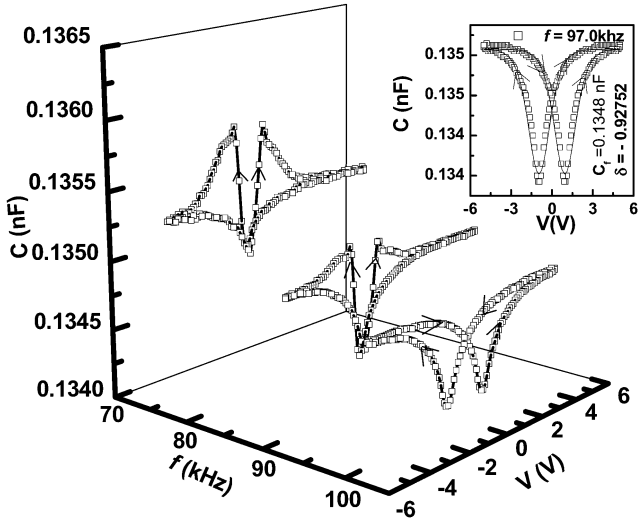


Figure 8. (*a*) *C–V* hysteresis curves for signal frequency (*f*) 70.0, 80.0 and 100.0 kHz, showing the gradual change in behaviour with increasing *f*. The d.c. bias swept from −5.0 to +5.0 V in steps of 0.1 V and then reversed. (*b*) *C–V* hysteresis loop at $f$=97.0 kHz which is symmetric corresponding to the point at zero bias. The solid line is the fitted line with equation (10) with β=−0.927.

further increase of signal frequency, the peaks exhibited by the *C–V* hysteresis are gradually converted, showing intermediate 'frustrated behaviour,' to a well for the signal frequency $f_i$=95.0 kHz (figure 8). Moreover, equation (6) is not followed in the frustrated region between peaks and well. At frequencies $f_i$ and $f_l$, $C_f$ changes considerably. It is important to note that not only the ferroelectric torque (as considered above) is responsible for the switching between two states ($\phi_0$ to $\pi-\phi_0$), but the dielectric torque may also cooperate with or counteract the ferroelectric torque during switching, and also stabilize the molecular axis in its final position after switching. At higher frequencies the dielectric torque increases more rapidly with increasing field [13] than does the ferroelectric torque, and it is known that the FLC molecules naturally try to align the largest permittivity component along the field. If the frequency of the electric field is too high, the component $\varepsilon_2$ does not couple with the spontaneous polarization $\mathbf{P}_s$; the molecule will remain in (or return to) the almost fully switched state and will not contribute to the non-linear part of the capacitance. Such behaviour is expected for frequencies where $\partial\varepsilon$ vanishes. Finally, the inversion of the *C–V* hysteresis is related to the inversion of $\partial\varepsilon$ [26] at higher frequencies, and the inverted *C–V* loops again follow equation (10) with change of sign of β (=−0.927) as shown in figure 8.

### 3.3. *Magnitude of admittance (G)-voltage hysteresis*

In the equivalent circuit for the SSFLC, as shown in figure 1 (*a*), $R_p$ and $C_p$ are, respectively, permanent resistor and capacitor due to the polymer layer. The polymer layer (area $A$, thickness $d_p$) has dielectric constant $\varepsilon_p=3.8$ and specific resistance $\rho=10^{14}\,\Omega\,m$ which give capacitance $C_p\approx10\,nF$ and resistance $R_p=3\times10^9\,\Omega$, respectively. The resistance $R_p$ can be ignored compared with the dynamical impedance of the polymer capacitor, as we are interested in frequencies $f>100\,mHz$ and the circuit becomes simpler as shown in figure 1 (*b*). Hence considering the FLC capacitor as a parallel combination of a capacitance and resistor, the value of conductance (magnitude of admittance, $G$) is given by

$$G=\left(\frac{1}{R^2}+\omega^2C^2\right)^{\frac{1}{2}}. \tag{11}$$

The $G$–$V$ hysteresis loops for the SSFLC at different frequencies (0.1, 0.5 and 1.0 kHz) are shown in figure 9. The peak height of the $G$–$V$ hysteresis loop increases with frequency; the linear part of the conductance of the hysteresis loops shows little increase with increasing frequency. Such behaviour is expected from equation (10) which shows that the conductance depends upon $\omega C$ as well as on the non-linear $R$ value of the equivalent circuit, figure 1 (*c*). Increase in the linear part of the conductance with frequency is due to the contribution from the ITO coating of the substrates, which increases with increasing frequency. Figure 10 clearly shows the increase in the peak height of the $\omega C$–$V$ loop with frequency, and hence equation (7) suggests the increase of peak height of $G$–$V$ hysteresis with frequency.

## 4. Conclusion

In a surface stabilized ferroelectric liquid crystal device, the rotational motion of the director around the smectic cone at a fixed temperature (~40°C, well below the SmA–SmC* transition temperature 62.0°C of the system CS-1027 under investigation) not only gives rise to the Goldstone mode but also effects the polarization reversal process. The amount of switchable polarization during polarization reversal is found to decrease with increasing frequency of the applied signal, as the traversal path of the director decreases. The observed inversion of the capacitance–voltage hysteresis at a characteristic higher frequency ($f_l$) in a FLC is attributed to the inversion of dielectric biaxiality at higher frequencies. The inversion frequency $f_i$ at a fixed temperature (~40°C) is much greater than the relaxation frequency $f_R$ at that temperature. The anomalous (frustrated) behaviour exhibited by the hysteresis loop within the frequencies between $f_l$ and $f_i$ arises due to the competition between ferroelectric and dielectric torques. The frequency-dependent behaviours of $C$–$V$ and $G$–$V$ hysteresis can be explained by considering the equivalent electrical circuit for the SSFLC capacitor. Further experimental (confirmation of inversion in the biaxiality by using conoscopy) and theoretical studies would be

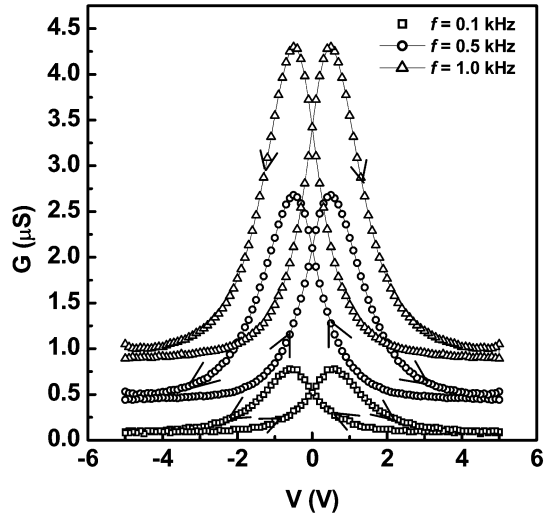


Figure 9. (*a*) Magnitude of admittance–voltage ($G$–$V$) hysteresis curves for signal frequency ($f$) 0.1, 0.2 and 1.0 kHz, showing the gradual increase in peak height of the $G$–$V$ hysteresis with increasing $f$. The d.c. bias swept from −5.0 to +5.0 V in steps of 0.1 V and then reversed.

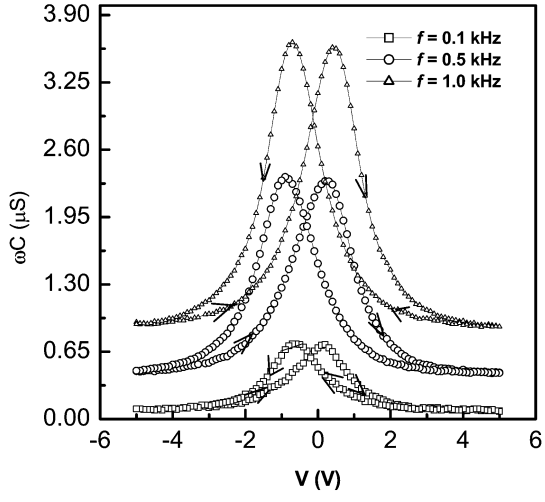


Figure 10. $\omega C$–$V$ hysteresis curves for signal frequency ($f$) 0.1, 0.2 and 1.0 kHz, showing the gradual increase in peak height of the $\omega C$–$V$ hysteresis with increasing $f$. The d.c. bias swept from −5.0 to +5.0 V in steps of 0.1 V and then reversed.

interesting for elucidation of the complete picture of the frequency- and temperature-dependent *C–V* hysteresis behaviour in a SSFLC cell.

**Acknowledgement**

The authors are grateful to the Council of Scientific and Industrial Research, Government of India, for financial support, and E. Okabe, Chisso Corporation, Japan for providing the FLC materials.

**References**

[1] R.B. Meyer, L. Liebert, L. Strzelecki, P.J. Keller. *J. Phys. (Paris) Lett.*, **36**, L-69 (1975).
[2] J. Hoffmann, W. Kuczynski, J. Malecki, J. Pavel. *Ferroelectrics*, **76**, 61 (1987).
[3] F. Gouda, W. Kuczynski, S.T. Lagerwall, M. Matuszczyk, T. Matuszczyk, K. Skarp. *Phys. Rev. A*, **46**, 951 (1992).
[4] F. Gouda, M. Buivydas, T. Carlsson, S.T. Lagerwall, B. Stebler. *Phys. Lett. A*, **190**, 345 (1994).
[5] C.V. Brown, J.C. Jones. *J. appl. Phys.*, **86**, 3333 (1999).
[6] N.A. Clark, S.T. Lagerwall. *Appl. Phys. Lett.*, **36**, 899 (1980).
[7] A. Levstik, T. Carlsson, C. Filipic, B. Zeks. *Mol. Cryst. liq. Cryst.*, **154**, 259 (1988).
[8] T.P. Rieker, N.A. Clark, G.S. Smith, D.S. Parmar, E.B. Sirota, C. Safinya. *Phys. Rev. Lett.*, **59**, 2658 (1987).
[9] A. Fukuda, G. Andersson, T. Carlsson, S. Lagerwall, T.K. Skarp, B. Stebler. *Mol. Cryst. liq. Cryst.*, **6**, 151 (1989).
[10] Y.P. Panarin, Y.P. Kalmykov, S.T. Mac Lughadha, H. Xu, J.K. Vij. *Phys. Rev. A*, **50**, 4763 (1994).
[11] J. Pavel, M. Glogarova, S.S. Bawa. *Ferroelectrics*, **76**, 221 (1987).
[12] C. Reynaerts, A. de Vos. *J. Phys. D*, **22**, 1504 (1989).
[13] F. Gouda, G. Anderson, M. Matuszczyk, K. Skarp, S.T. Lagerwall. *J. appl. Phys.*, **67**, 180 (1990).
[14] P. Yang, D.L. Carroll, J. Ballato, R.W. Schwartz. *Appl. Phys. Lett.*, **81**, 4583 (2002).
[15] S.L. Miller, R.D. Nasby, J.R. Schwank, M.S. Rodgers, P.V. Dressendorfer. *J.appl. Phys.*, **68**, 6462 (1990); S.L. Miller, J.R. Schwank, R.D. Nasby and M.S. Rodgers. *J. appl. Phys.*, **70**, 2849 (1991).
[16] N. Bar-Chaim, M. Brunstein, J. Grunberg, A. Seidman. *J. Appl. Phys.*, **45**, 2398 (1978).
[17] I. Mayergoyz. *Mathematical Models of Hysteresis*. Springer, New York (1991).
[18] D. Rep, M. Prins. *J. appl. Phys.*, **85**, 7923 (1999).
[19] C.B. Sawyer, C.H. Tower. *Phys. Rev.*, **35**, 269 (1930).
[20] K. Yoshino, T. Uemoto, Y. Inuishi. *Jpn. J. appl. Phys.*, **16**, 571 (1977).
[21] K.S. Cole, R.H. Cole. *J. chem. Phys.*, **9**, 341 (1941).
[22] S.U. Vallerien, F. Kremer, B. Hueser, H.W. Spieβ. *Colloid polym. Sci.*, **267**, 583 (1989).
[23] T.P. Reiker, N.A. Clark, G.S. Smith, D.S. Parmar, E.B. Sirota, C.R. Safinya. *Phys. Rev. Lett.*, **59**, 2658 (1987).
[24] S.L. Miller, J.R. Schwank, R.D. Nasby, M.S. Rodgers. *J. appl. Phys.*, **70**, 2849 (1991).
[25] C. Kuhn, H. Honigschmid, O. Kowarik, E. Gondro, K. Hoffman, 12th IEEE International Symposium on the Application of Ferroelectrics, Honululu, Hawaii, July, 2000 (unpublished).
[26] N. Itoh, M. Koden, S. Miyoshi, T. Akahane. *Liq. Cryst.*, **18**, 109 (1995).